microbial biotechnology

Open Access

High ambient temperature exposure during late gestation disrupts glycolipid metabolism and hepatic mitochondrial function tightly related to gut microbial dysbiosis in pregnant mice

Jianwen He,[1,2] Riliang Liu,[1] Weijiang Zheng,[1] Huiduo Guo,[1] Yunnan Yang,[1] Ruqian Zhao[3] and Wen Yao[1,3]

[1]*College of Animal Science and Technology, Nanjing Agricultural University, Nanjing, 210095, China.*
[2]*Affiliated Hospital of Shaanxi University of Chinese Medicine, Shaanxi University of Chinese Medicine, Xianyang, 712000, China.*
[3]*Key Lab of Animal Physiology and Biochemistry, Nanjing Agricultural University, Ministry of Agriculture and Rural Affairs of the People's Republic of China, Nanjing, 210095, China.*

Summary

As global warming intensifies, emerging evidence has demonstrated high ambient temperature during pregnancy negatively affects maternal physiology with compromised pregnant outcomes; however, little is known about the roles of gut microbiota and its underlying mechanisms in this process. Here, for the first time, we explored the potential mechanisms of gut microbiota involved in the disrupted glycolipid metabolism via hepatic mitochondrial function. Our results indicate heat stress (HS) reduces fat and protein contents and serum levels of insulin and triglyceride (TG), while increases that of non-esterified fatty acid (NEFA), β-hydroxybutyric acid (B-HBA), creatinine and blood urea nitrogen (BUN) ($P < 0.05$). Additionally, HS downregulates both mitochondrial genes (mtDNA) and nuclear encoding mitochondrial functional genes with increasing serum levels of malondialdehyde (MDA) and 8-hydroxydeoxyguanosine (8-OHdG) ($P < 0.05$). Regarding microbial response, HS boosts serum levels of lipopolysaccharide (LPS) ($P < 0.05$) and alters β-diversity (ANOSIM, $P < 0.01$), increasing the proportions of *Escherichia–Shigella*, *Acinetobacter* and *Klebsiella* ($q < 0.05$), while reducing that of *Ruminiclostridium*, *Blautia*, *Lachnospiraceae_NK4A136_group*, Clostridium VadinBB60 and Muribaculaceae ($q < 0.05$). PICRUSt analysis predicts that HS upregulates 11 KEGG pathways, mainly including bile secretion and bacterial invasion of epithelial cells. The collective results suggest that microbial dysbiosis due to late gestational HS has strong associations with damaged hepatic mitochondrial function and disrupted metabolic profiles.

Introduction

Global ambient temperatures are steadily rising, and climate change-related health problems have soared (Koh, 2016; NOAA, 2020). A growing body of studies has linked higher ambient temperature with colossal economic losses and detrimental health outcomes, including mortality, morbidity, infectious disease and mental health (Ma *et al*., 2015; Yang *et al*., 2015; Hsiang *et al*., 2017). Pregnant women, especially during late gestation, are much more vulnerable to heat compared with the non-pregnant since their basal metabolic rate increases by 20–30% to meet the energy requirements of fetal rapid growth and development (Lof *et al*., 2005; Strand *et al*., 2011). Previous studies have revealed that high ambient temperature adversely impacts both maternal metabolism and offspring development, including pregnant complications such as preeclampsia and eclampsia (Beltran *et al*., 2014; Nasiri *et al*., 2014), as well as preterm birth, miscarriage, low birthweight and even teratogenesis (Strand *et al*., 2011; Kilinc *et al*., 2016; Basu *et al*., 2017; Zhang *et al*., 2017).

High ambient temperature easily generates heat stress (HS), which is reported to be cytotoxic since it can induce cell oxidative damage and activate programmed cell apoptosis (Du *et al*., 2008). As the organelle produces the most reactive oxygen species (ROS), mitochondria bear the brunt of oxidative damage when the concentration of ROS is too high. Meanwhile, their respiratory chain complex enzymes I (NADH dehydrogenase), II (succinate dehydrogenase), IV (cytochrome c oxidase) and V (ATP synthase) are inactivated by ROS, resulting

Received 10 April, 2021; accepted 3 July, 2021.
For correspondence. E-mail yaowen67jp@njau.edu.cn; Tel. +86 025 84399830; Fax +86 025 84399830.
Microbial Biotechnology (2021) **14**(5), 2116–2129
doi:10.1111/1751-7915.13893

in reduced respiratory chain electron transfer, ATP synthesis and cell energy supply (Diebold and Chandel, 2016). Moreover, HS changes the mitochondrial histological morphology and internal structure, causing mitochondria swelling, cristae rupture and matrix density reduction (Lu *et al*., 2017). Mujahed also points out that HS induces lipid peroxidation and protein denaturation of muscle mitochondria (Mujahid *et al*., 2007b). Mitochondrial damage induced by HS may be the reason why cells cannot meet the energy requirements of humans and animals. Additionally, insufficient energy supply may lead to disrupted glycolipid metabolism, which is associated with preterm birth and even stillborn in pregnancy (Gao et al., 2021; Abrams, 2021).

The mammalian gastrointestinal (GI) tract hosts trillions of microorganisms, which are the same size as somatic cells but possess more genes and metabolic pathways (Krautkramer *et al*., 2020). Accumulating evidence has revealed that gut microbiota plays an essential role in maintaining the host physiological homeostasis, regulating host metabolism and promoting immune system development (Nicholson *et al*., 2012; Sommer and Bäckhed, 2013). The previous study has shown that HS stimulates blood transfer from internal organs to the skin via gastrointestinal vasoconstriction and peripheral vasodilation, causing hypoxic stress and increased permeability of the intestinal epithelium, further leading to endotoxaemia, inflammation and even organ damage (Lambert, 2009). However, the HS influence during pregnancy on the maternal gut microbiota is rarely reported. Our previous study indicates that late gestational HS causes profound changes in the gut microbial composition in a pig model, especially in some short-chain fatty acids (SCFAs) producing species. These bacteria subsequently alter the SCFA formation and nitrogen degradation and further influence the gut homeostasis and inflammatory response (He *et al*., 2019a). Intriguingly, according to the endosymbiotic theory, the mitochondria are considered as the evolutionary descendant of the bacterial cells (Bajpai *et al*., 2018). Also, the mitochondrial respiratory chain retains the bacterial characteristic that using fumarate as an alternative electron acceptor during hypoxia (Sridharan *et al*., 2008), which implies the possibility that its function might be regulated by microbial metabolites. However, as far as we have known, no study focuses on the potential mechanisms of gut microbiota involved in the disrupted glycolipid metabolism during late gestational HS via hepatic mitochondrial function.

To this end, we used a mouse as the model in our study for HS treatment from 12 to 18 days of gestation. We first observed the changes in both maternal physiological status (temperature, feed intake, water consumption) and metabolic profiles (body composition and serum metabolic parameters). Afterwards, HS effects on the mitochondrial function and microbial structure are investigated by mRNA expressions of liver mitochondrial functional genes and 16S rRNA gene sequencing respectively. Finally, the random forest algorithm and multiple linear regression are used to predict the contribution of potential microbial drivers for mitochondrial function and metabolic profiles. Taken together, the present study as a pioneering work provides evidence high ambient temperature exposure disrupts glycolipid metabolism and hepatic mitochondrial function in pregnant mice, which is strongly associated with gut microbial dysbiosis.

Results

Establishment of HS model

To ensure the pregnant mice were exposed to environmental HS, we firstly explored whether the HS model was established in this study. Our results showed that serum levels of heat shock protein 70 (Hsp70), corticotropin-releasing hormone (CRH), adrenocorticotropic hormone (ACTH) and corticosterone (Fig. S1A–D; $P < 0.001$) were all increased due to HS, indicating that the hypothalamic–pituitary–adrenal (HPA) axis was activated, and the HS model was established successfully.

Rectal temperature, feed intake and water consumption

The rectal temperature increased and tended to increase owing to HS only at gestational day (GD) 16 (Fig. S2A; $P < 0.0001$) and GD17 (Fig. S2A; $P < 0.10$) respectively. Unlike rectal temperature, feed intake and water consumption were changed immediately. Feed intake was reduced immediately when HS treatment was implemented at GD12 (Fig. S2B; $P < 0.0001$) and then it increased at GD13-15, but still lower than that of the thermoneutral (TN) group until GD16 (Fig. S2B; $P < 0.0001$). Water consumption increased suddenly when HS treatment was operated at GD12, and this difference persisted until delivery (Fig. S2C; $P < 0.05$). Moreover, an interaction between HS treatment and the pregnancy was found in all three parameters ($P < 0.05$).

Body weight, body composition and visceral index

As regards body weight, there was an interaction between HS treatment and the pregnancy (Fig. 1A; $P < 0.01$), although no significant difference was observed in the two groups. Body weight increased at neither GD12-13 nor GD15-16 owing to HS, indicating HS treatment suppressed body weight gain during the pregnancy. Further, the declined serum insulin-like

growth factor-1 (IGF-1) level also supported the suppressive growth in the HS group (Fig. 1B; $P < 0.05$). Additionally, HS decreased and tended to reduce the carcass fat and protein content respectively (Fig. 1C; $P < 0.05$). Especially, the visceral index of abdominal fat was reduced notably due to HS (Fig. 1D; Table S1; $P < 0.01$).

Serum metabolic parameters

Serum metabolism was affected as shown in Table 1. As regards carbohydrate, HS reduced insulin level ($P < 0.001$), while increased that of glucagon ($P < 0.05$). Regarding lipid, HS decreased triglyceride (TG) level ($P < 0.01$), while elevated that of non-esterified fatty acid (NEFA) ($P < 0.001$) and β-hydroxybutyric acid (B-HBA) ($P < 0.01$). Concerning protein, blood urea nitrogen (BUN) ($P < 0.01$) and creatinine ($P < 0.001$) levels were increased due to HS. Additionally, the concentrations of malondialdehyde (MDA) ($P < 0.001$) and 8-hydroxy-2 deoxyguanosine (8-OHdG) ($P < 0.05$) were also elevated owing to HS. Our results showed that HS stimulated negative energy balance (NEB) and oxidative damage of pregnant mice, leading to intensified catabolism of fat and protein.

Hepatic mRNA changes related to mitochondrial function

The mRNA expressions of 10 out of 13 mitochondrial genes (mtDNA) encoded genes involved in oxidative phosphorylation (OxPhos) were downregulated due to HS (Fig. 2A; $P < 0.05$). Additionally, nuclear-encoded genes involved in mitochondrial biogenesis, thermogenesis, fatty acid β-oxidation and tricarboxylic acid cycle (TCA) cycle were also decreased (Fig. 2B; $P < 0.05$), such as mitochondrial transcription factor A (TFAM), uncoupling protein 2 (UCP2), carnitine palmitoyltransferase 1α (CPT-1α) and citrate synthase (CS). Our results suggested that late gestational HS declined mRNA expressions of hepatic mitochondrial functional genes, thus affecting the OxPhos and substrate oxidation efficiency.

Table 1. Effects of HS during late gestation on serum metabolic parameters of pregnant mice.

	Item TN	Treatments HS	*P*-value
n	10	8	–
Glucose, mM	5.06 ± 0.40	4.25 ± 0.34	NS
Insulin, mIU l^{-1}	36.59 ± 1.26	24.94 ± 1.41	<0.001
Glucagon, ng l^{-1}	146.37 ± 8.61	182.15 ± 10.95	<0.05
Cholesterol, mM	1.90 ± 0.10	1.61 ± 0.14	NS
Triglyceride, mM	2.07 ± 0.13	1.36 ± 0.13	<0.01
HDL, mM	0.67 ± 0.06	0.64 ± 0.07	NS
LDL, mM	0.42 ± 0.04	0.39 ± 0.02	NS
NEFA, μM	534.98 ± 24.54	714.23 ± 16.98	<0.001
B-HBA, μM	281.30 ± 14.71	405.43 ± 27.86	<0.01
Creatinine, μM	121.99 ± 5.70	183.86 ± 5.28	<0.001
BUN, mM	9.46 ± 0.97	13.96 ± 0.93	<0.01
MDA, nmol ml^{-1}	23.37 ± 1.01	29.91 ± 1.08	<0.001
8-OHdG, ng ml^{-1}	38.32 ± 2.19	45.10 ± 1.93	<0.05

HS, heat stress; NS, not significant ($P > 0.10$); TN, thermoneutral. Data are presented as the mean ± SEM.

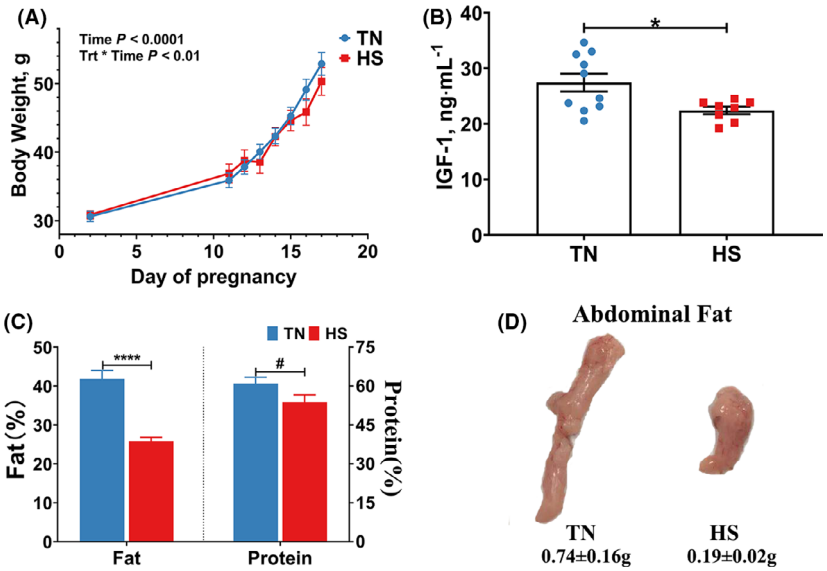

Fig. 1. Effects of HS during late gestation on the body weight (A–B) and body composition (C–D) of pregnant mice. The data are presented as the mean ± SEM. Asterisks (#, *, ****) mean the tendency or significant difference between TN and HS groups ($P < 0.10$, $P < 0.05$, $P < 0.0001$). HS, heat stress; IGF-1, insulin-like growth factor-1; TN, thermoneutral.

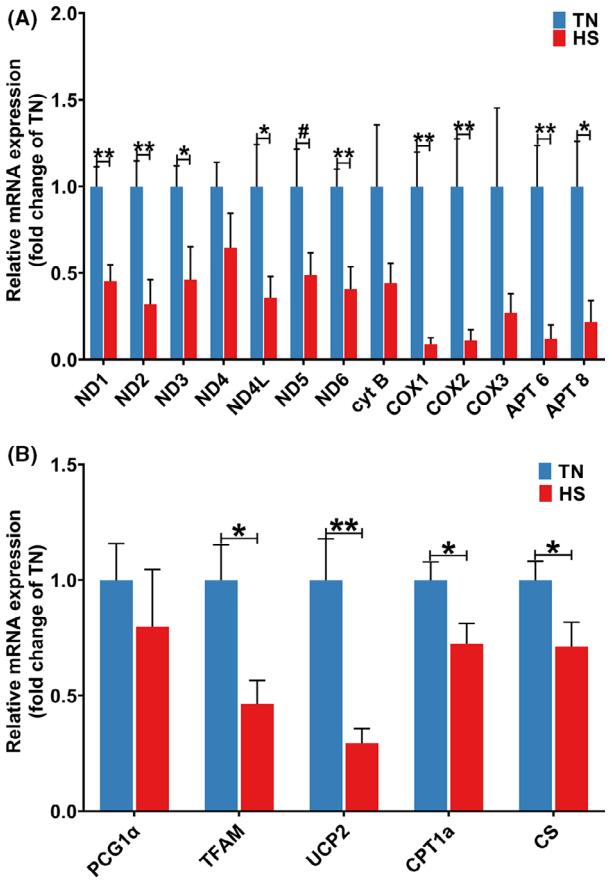

Fig. 2. Effects of HS during late gestation on the relative mRNA gene expressions of mtDNA-encoded (A) and mitochondrial functional (B) genes in pregnant mice liver. The data are presented as the mean ± SEM. Asterisks (#, *, **) mean the tendency or significant difference between TN and HS groups ($P < 0.10$; $P < 0.05$; $P < 0.01$). CPT1α, carnitine palmitoyltransferase-Iα; CS, citrate synthase; HS, heat stress; PCG1α, peroxisome proliferator-activated receptor γ coactivator-Iα; TFAM, mitochondrial transcription factor A; TN, thermoneutral; UCP2, uncoupling protein 2.

Colonic microbial diversity, composition and functional prediction

HS increased serum levels of lipopolysaccharide (LPS) and lipopolysaccharide-binding protein (LBP) (Fig. S3; $P < 0.05$), indicating gut permeability or microbiota may be altered. To explore HS effects on the microbial composition, we collected 18 samples from two groups and sequenced the bacterial 16S rDNA using Illumina MiSeq PE250. 730,640 high-quality sequences were classified as being bacteria with an average length of 420 bp. No effects were observed on the bacterial α-diversity due to HS, including richness estimators (ACE and Chao1), and diversity indices (Shannon and Simpson) (Table S3). There was, however, a significant alteration in the bacterial β-diversity. Principal coordinate analysis (PCoA) plot based on the unweighted_unifrac distance metric showed that the colonic bacterial communities were separated thoroughly by HS (Fig. 3A; ANOSIM, $P = 0.005$; Adonis, $P = 0.01$).

Regarding microbial composition, at the phylum level, Bacteroidetes and Firmicutes were the most predominant phyla in the colon, with a total relative abundance above 90%. The following ranks are phyla Deferribacteres, Proteobacteria and Verrucomicrobia (Fig. 4B). HS boosted the proportion of Proteobacteria (Fig. 3B; $q < 0.01$). At the OTU level, we constructed a phylogenetic tree of differential OTU and observed a total of 22 OTU that belonging to 8 different families or genera (Fig. 3C). OTU related to genera *Escherichia–Shigella*, *Acinetobacter* and *Klebsiella* was enriched in the HS group. The rest of OTU is related to family or genera Muribaculaceae, Clostridium VadinBB60, *Ruminiclostridium*, *Blautia* and *Lachnospiraceae_NK4A136_group* were almost enriched in the TN group.

Using PICRUSt as a predictive exploratory tool, we found that late gestational HS impacted colonic bacterial functions via 69 KEGG pathways (Table S4). Among them, HS upregulated 11 KEGG pathways, including bile secretion, bacterial invasion of epithelial cells, staphylococcus aureus infection, RIG-I-like receptor signalling pathway, biosynthesis of siderophore group nonribosomal peptides, geraniol degradation, α-linolenic acid metabolism, arachidonic acid metabolism, metabolism of xenobiotics by cytochrome P450, chlorocyclohexane and chlorobenzene degradation and phosphotransferase system (PTS) (Fig. 3D; log2 fold change>0.585, $P < 0.05$). These upregulated pathways were related to the digestive system, infectious diseases, immune system, metabolism of terpenoids and polyketides, lipid metabolism, xenobiotics biodegradation and metabolism, and membrane transport (Fig. 3D).

Potential bacterial drivers of serum metabolic profiles and hepatic mitochondrial functions

As differential bacteria, family Muribaculaceae and Clostridiales VadinBB60, and genera *Escherichia–Shigella*, *Acinetobacter*, *Klebsiella*, *Ruminiclostridium*, *Blautia* and *Lachnospiraceae_NK4A136_group* were serving as the candidates for potential bacterial drivers. Concerning serum metabolic profiles, (i) *Ruminiclostridium* ($P < 0.01$), *Escherichia–Shigella* and *Klebsiella* ($P < 0.05$) contributed to the CRH level (Fig. 4A); (ii) *Acinetobacter* ($P < 0.001$), *Klebsiella* and *Ruminiclostridium* ($P < 0.01$) contributed to the ACTH level (Fig. 4B); (iii) Clostridiales VadinBB60 and *Ruminiclostridium* contributed to the corticosterone level (Fig. 4C; $P < 0.05$); (iv) *Ruminiclostridium* and *Klebsiella* ($P < 0.05$) and *Escherichia–Shigella* and *Acinetobacter* ($P < 0.10$) contributed to the insulin level (Fig. 4D); (v)

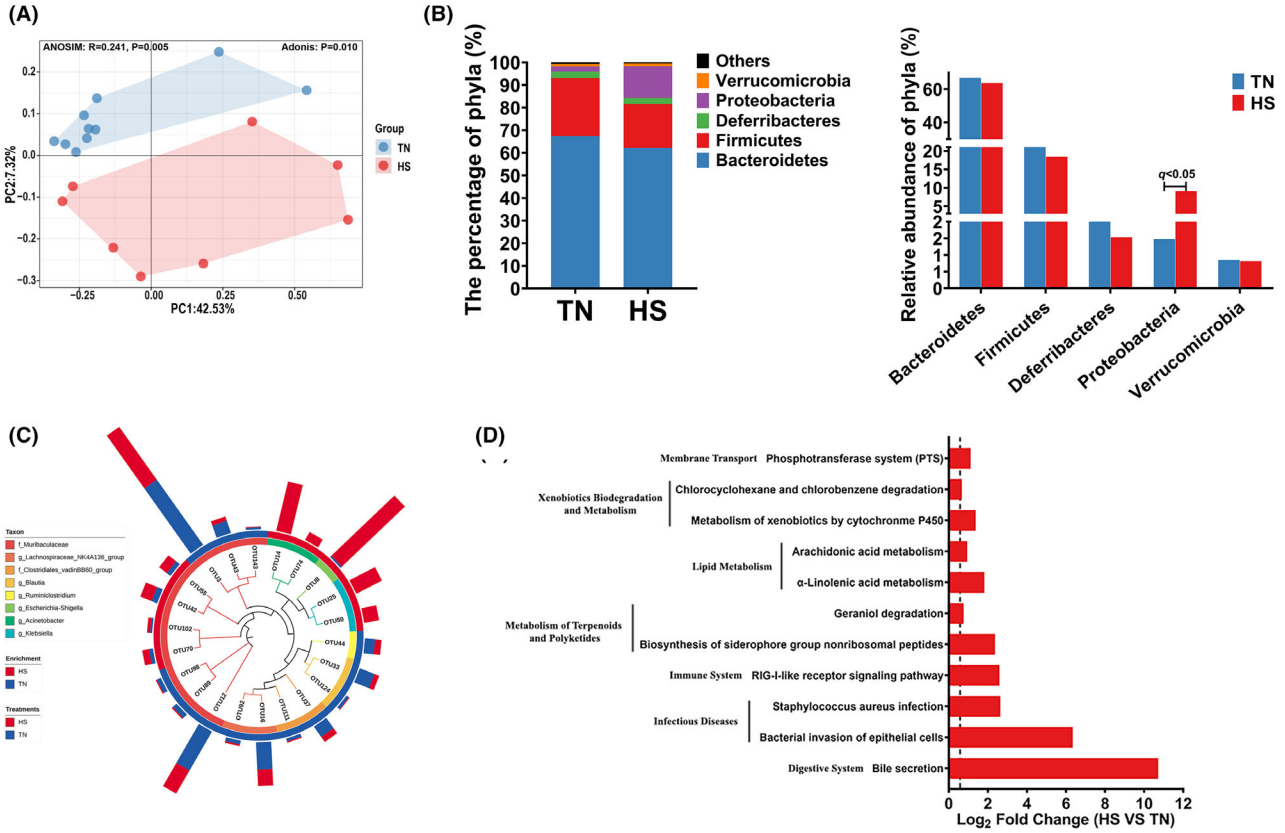

Fig. 3. Effects of HS during late gestation on colonic microbial β-diversity (A), composition (B–C) and KEGG pathways (D) of pregnant mice. (A) Principal coordinate analysis (PCoA) plot of colonic bacteria based on the unweighted_unifrac distance metric of OTU. Bacterial community structure comparisons were evaluated by permutational multivariate analysis of variance (PERMANOVA), and $P < 0.05$ indicates a significant difference. (B) The data are presented as medians, and $q < 0.05$ indicates a significant difference. (C) The iTOL plot shows the phylogenetic tree of significant dominant OTU and their relative abundance and enrichment of colonic bacteria. (D) The data are presented as log2 fold change, and log2 fold change >0.585 indicates a significant upregulation. HS, heat stress; iTOL, interactive tree of life; KEGG, Kyoto Encyclopedia of Genes and Genomes; TN, thermoneutral.

Ruminiclostridium, *Klebsiella* ($P < 0.05$) and *Escherichia–Shigella* ($P < 0.10$) contributed to the NEFA level (Fig. 4E); (vi) *Ruminiclostridium* ($P < 0.01$) and *Klebsiella* ($P < 0.05$) contributed to the BUN level (Fig. 4F); (vii) Clostridiales VadinBB60, *Ruminiclostridium* and *Escherichia–Shigella* tended to contribute to the creatinine level (Fig. 4G; $P < 0.10$); (viii) *Ruminiclostridium* and *Acinetobacter* contributed to the LPS level (Fig. 4H; $P < 0.05$); and (ix) *Ruminiclostridium, Escherichia–Shigella* and *Klebsiella* contributed to the LBP level (Fig. 4I; $P < 0.05$). Our results implied that the decreased relative abundance of *Ruminiclostridium*, as well as increased proportion of *Klebsiella* and *Escherichia–Shigella*, was acting as the potential drivers of serum metabolic profiles.

As regards liver mitochondrial functions, *Ruminiclostridium* ($P < 0.01$), *Escherichia–Shigella* ($P < 0.05$) and Muribaculaceae ($P < 0.10$) contributed to the ND4L mRNA expression (Fig. 5A); *Ruminiclostridium* and *Klebsiella* ($P < 0.001$), Clostridiales VadinBB60, *Escherichia–Shigella* and Muribaculaceae ($P < 0.01$) and *Acinetobacter* ($P < 0.05$) contributed to the COX1 mRNA expression (Fig. 5B); and only *Escherichia–Shigella* ($P < 0.10$) or Muribaculaceae ($P < 0.05$) contributed to the mRNA expression of CTP1 or UCP2 (Fig. 5C and D) respectively. Our results suggested that colonic microbiota, especially *Ruminiclostridium* and *Escherichia–Shigella*, were more likely to affect the mRNA expression of mitochondrial encoding genes.

Discussion and conclusions

Currently, the HS impacts on the physiological and metabolic profiles of the gestational animal model have been illustrated sufficiently (Gonzalez-Rivas *et al.*, 2019). We have pointed out that late gestational HS induces maternal gut microbial dysbiosis which is transferred to her offspring in a pig model (He *et al.*, 2020). Emerging evidence indicates a robust association between the gut microbiota, especially its metabolites, and liver

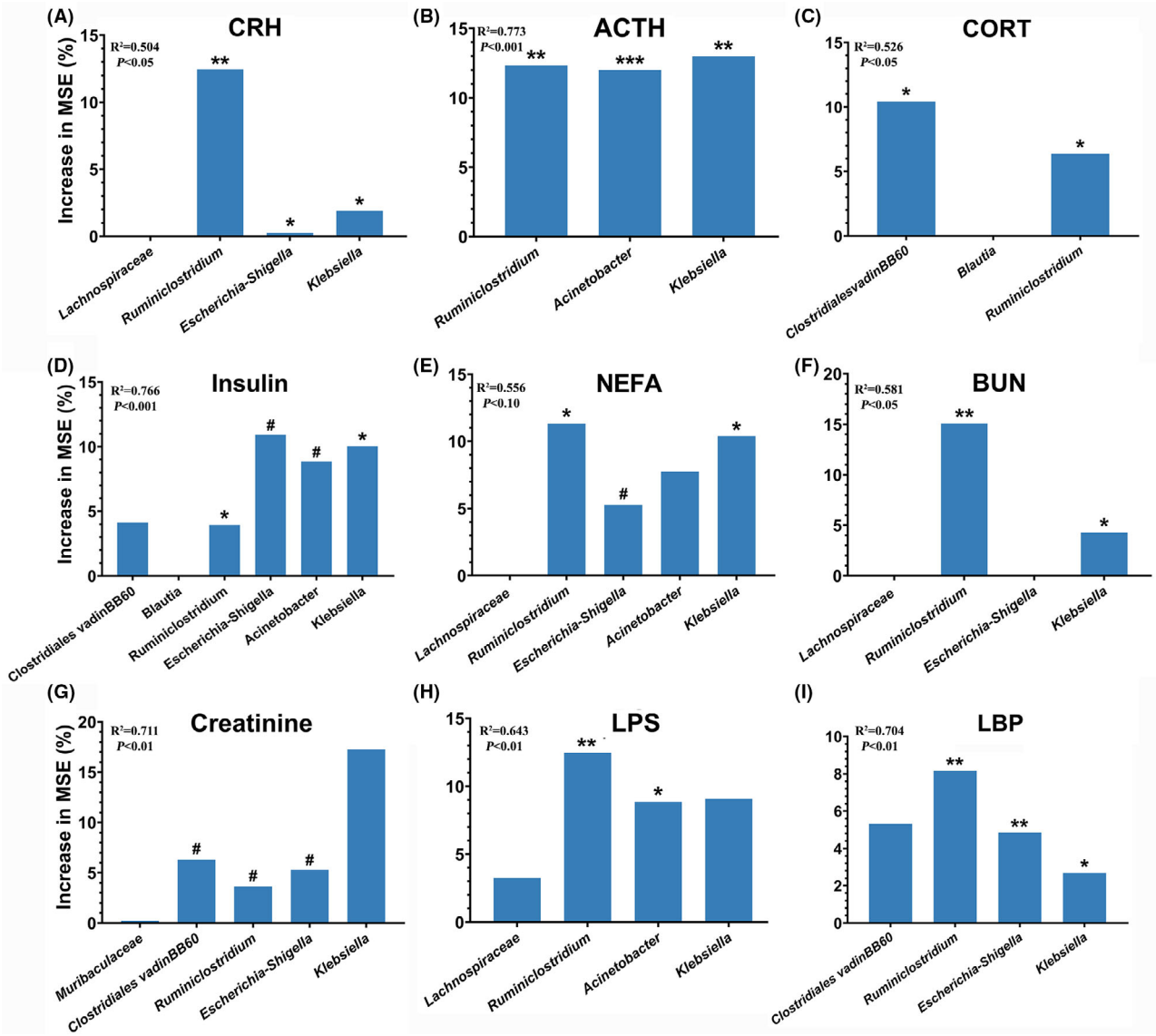

Fig. 4. potential bacterial drivers of serum metabolic profiles and hepatic mitochondrial functions. (A-C) For HPA axis hormones. (D-G). For lipid and protein metabolism. (H-I) For intestinal integrity. Percentage increases in the MSE of variables were used to estimate the importance of these predictors, and higher MSE% values imply more important predictors. The data are analysed by the RF package and lm and relwight function in R. Asterisks (#, *, **, ***) mean the tendency or significant difference between TN and HS groups ($P < 0.10$; $P < 0.05$; $P < 0.01$; $P < 0.001$). HPA, hypothalamic pituitary adrenal; MSE, mean squared error; RF, random forest.

dysfunction (Compare *et al*., 2012). However, the underlying relationship between gut microbiota and hepatic mitochondrial function involved in the HS physiological response is truly lacking. Here, we firstly investigate the potential mechanisms of gut microbiota involved in the disrupted glycolipid metabolism during late gestational HS via hepatic mitochondrial function in a mouse model. The increased levels of CRH, ACTH, corticosterone and Hsp70 indicate the activation of the HPA axis and the established HS model, which is consistent with our results in a pig model (He *et al*., 2019b). As regards physiological response, HS elevates rectal temperature and water consumption, while reduces feed intake as previous studies reported (Harikai *et al*., 2003; Morera *et al*., 2012; Aggarwal and Upadhyay, 2012). The reduced feed intake or feed efficiency may be related to decreased appetite or basal metabolic rate for alleviating HS (He *et al*., 2018). Regarding metabolic profiles, HS reduces serum concentration of insulin and triglyceride, while increases that of glucagon, NEFA, B-HBA, creatinine and BUN. Decreased insulin and increased glucagon indicate enhanced catabolism (Sharma *et al*., 2018;

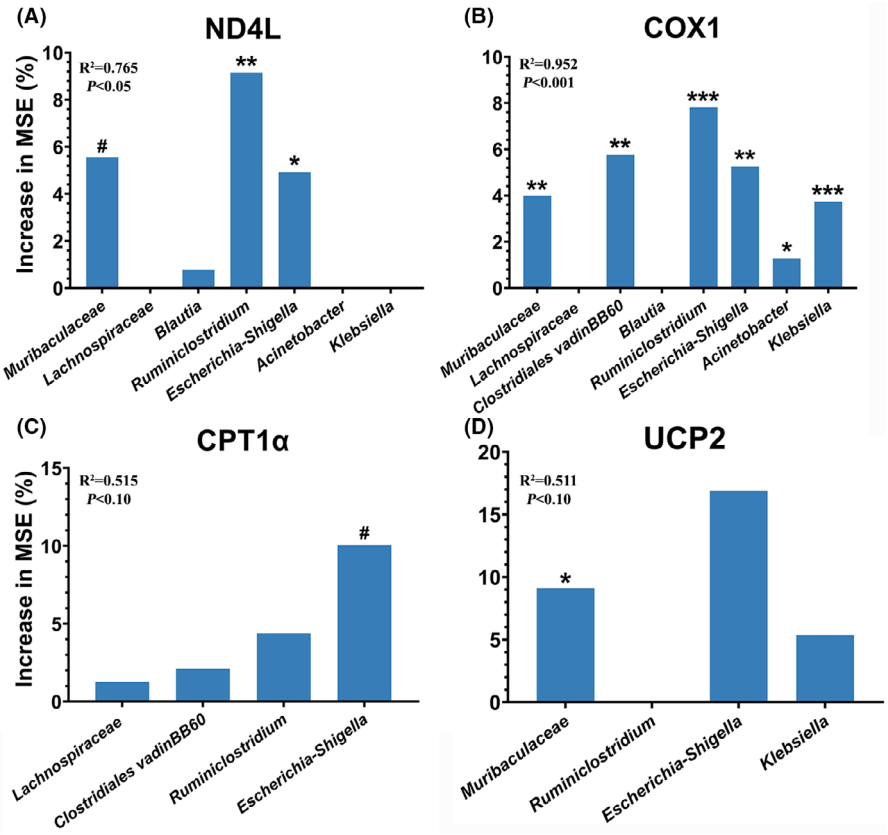

Fig. 5. Potential microbial drivers (relative abundance of colonic differential bacteria) of variations in relative mRNA expression of liver mitochondrial functional genes of pregnant mice. (A-B) For mtDNA encoding mitochondrial functional genes. (C-D) For nuclear encoding mitochondrial functional genes. Percentage increases in the MSE of variables were used to estimate the importance of these predictors, and higher MSE% values imply more important predictors. The data are analysed by the RF package and lm and relwight function in R. Asterisks (#, *, **, ***) mean the tendency or significant difference between TN and HS groups ($P < 0.10$; $P < 0.05$, $P < 0.01$; $P < 0.001$). mtDNA, mitochondrial genes; MSE, mean squared error; RF, random forest.

Galsgaard *et al*., 2019). The elevated NEFA and B-HBA levels suggest aggravated hepatic fat decomposition and abnormal lipid metabolism (Xue *et al*., 2019), which is also supported by the reduced carcass fat content and abdominal fat index in our study. Further, increased creatinine and BUN levels also show exacerbated protein decomposition (Pearce *et al*., 2013; Liao *et al*., 2018). Our metabolism results indicate that HS stimulates negative energy balance and intensifies fat and protein catabolism of pregnant mice.

The liver is the largest parenchymatous organ that governs whole-body energy metabolism, including energy production, storage, release and substrates for further utilization (Papacleovoulou *et al*., 2017). Moreover, it is well established that the liver acts as the first sensor and processor to deliver maternal nutrients to a growing fetus via the umbilical vein (Zhou *et al*., 2019). Therefore, the liver plays a crucial role in energy metabolism and nutrient transport during pregnancy. Further, mitochondria are the most important organelles for energy metabolism. Mitochondria are the places where sugars, fats and amino acids are finally oxidized to release energy (Nelson and Cox, 2017). The mtDNAs primarily encode the respiratory chain complex enzymes of the mitochondrial inner membrane. Specifically, ND (1-6) genes encode the complex enzyme I (NADH dehydrogenase), CytB gene encodes the complex enzyme III (Q-cytochrome c reductase), COX (1-3) genes encode the complex enzyme IV (cytochrome c oxidase), and ATP genes encode complex V (F_1F_0ATP synthase) (Bellance *et al*., 2009). HS downregulates the mRNA expression of mtDNA in our study, indicating HS may impede the mitochondrial respiratory chain efficiency, resulting in reduced OxPhos and insufficient energy supply of cells. mtDNA is more vulnerable to ROS attack than nuclear DNA because of its closed position to the respiratory chain and lacking protective histone and effective DNA repair mechanism (Cadenas and Davies, 2000). The increasing serum 8-OHdG and MDA levels may also imply HS inhibits mitochondrial OxPhos by mainly

promoting mtDNAs oxidative damage (Belhadj Slimen *et al*., 2016). Additionally, mtDNA's replication, transcription and protein synthesis are dependent on the synergistic effects of various protein factors encoded by nuclear DNA as well (Liu and Li, 2009). HS decreases the mRNA expression of nuclear coding genes TFAM, UCP2, CPT1a and CS in this study. TFAM regulates mtDNA's replication and transcription (Farge *et al*., 2014), and its decreased level indicates suppressive mitochondrial biosynthesis. UCP2 is a transporter located in the inner membrane of mitochondria, which transports protons from the intermembrane space into the mitochondrial matrix for reducing both ATP and ROS levels in the mitochondria (Mailloux and Harper, 2011). The declined UCP2 level indicates cells are trying to increase ATP synthesis efficiency for alleviating deficient energy supply owing to HS but may be associated with boosted ROS level and aggravated oxidative damage (Echtay *et al*., 2002). This is consistent with Mujahid's report that HS promotes mitochondrial ROS production by downregulating the mRNA expression of the avUCP gene (Mujahid *et al*., 2007a). CPT1α and CS are two key enzymes for regulating β-oxidation and the TCA cycle respectively (Shi and Jiang, 2009). Their lessened mRNA expressions in the HS group indicate mitochondrial functions are impaired while affecting the oxidation efficiency of fatty acids and glucose as substrates (Lu *et al*., 2017). Hence, we speculate that late gestational HS may trigger mitochondrial damage for reducing carbohydrate and lipid oxidation efficiency while promoting fat and protein catabolism, thus altering body composition.

HS boosts serum levels of LPS and LBP in pregnant mice, which is consistent with our previous results in pregnant sows (He *et al*., 2019a), indicating intestinal integrity damage and inflammation. Alterations of intestinal integrity and immune status may be associated with the changes of gut microbiota (Karl *et al*., 2018). Our microbial data show that HS changes bacterial β-diversity, namely HS alters the bacterial structure of two groups. Consistent with Gohir's report (Gohir *et al*., 2015), Bacteroides and Firmicutes are the two principal phyla of pregnant mice, accounting for more than 90% of the relative abundance. The following rank is Deferribacteres, Proteobacteria and Verrucomicrobia. The microbial composition analysis indicates that HS decreases the relative abundance of OTU related to *Ruminiclostridium*, *Blautia*, *Lachnospiraceae_NK4A136_group*, Clostridiales VadinBB60 and Muribaculaceae. *Ruminiclostridium* belongs to Ruminococcaceae, while *Blautia* and *Lachnospiraceae_NK4A136_group* are the numbers of Lachnospiraceae. Ruminococcaceae and Lachnospiraceae are not only the key producing bacteria of SCFAs that playing a crucial role in gut development, health and homeostasis maintenance (Biddle *et al*., 2013; Li *et al*., 2019; Liu *et al*., 2019), but also the major producers of secondary bile acid (BAs) via 7 α/β decarboxylations to maintain bile acid homeostasis (Kakiyama *et al*., 2013). The PICRUSt predicts that HS strengthens the KEGG pathway of bile acid secretion, which also supports that HS affects bile acid metabolism via altering the gut bacterial composition. Augmented bile acid secretion during pregnancy can easily cause cholestasis of pregnancy that exerts long-term effects on the progeny especially metabolic syndrome (Mella *et al*., 2016). Muribaculaceae is originally Bacteroides S24-7, which is the dominant family in the gut of mice (Ormerod *et al*., 2016). In our study, the relative abundance of Muribaculaceae in the TN group and HS group is 57.41% and 50.81% respectively. Lagkouvardos et al. elucidate that there are at least eight different Muribaculaceae bacteria in the gastrointestinal (GI) tract of mice, which work together to degrade various carbohydrates (α-glycosides, host and plant glycosides) and nitrogen compounds (urea and cyanate esters) (Lagkouvardos *et al*., 2019). The PICRUSt also predicts that HS enhances the KEGG pathways of xenobiotics biodegradation and metabolism. Additionally, HS elevates the proportion of Proteobacteria (2.27% vs. 14.01%), especially in *Escherichia–Shigella*, *Acinetobacter* and *Klebsiella*. Boosted Proteobacteria during late gestation is closely related to gut microbial imbalance and aggravated inflammation (Koren *et al*., 2012). The PICRUSt also forecasts that HS heightens the KEGG pathways of bacterial invasion of epithelial cells, *staphylococcus aureus* infections and RIG-I-like receptor signalling. The increased bacterial invasion of epithelial cells and *staphylococcus aureus* infections are associated with impaired intestinal barrier function and aggravated intestinal bacterial inflammation (Hauck and Ohlsen, 2006). The RIG-I-like receptor is a pattern recognition receptor that specifically recognizes viral expression, which strengthening indicates the risk of viral infection due to HS (Yoneyama and Fujita, 2009). Our microbial results imply that HS exacerbates metabolic disorder and inflammatory response via altering gut microbiota during pregnancy.

Regarding potential microbial drivers, reduced *Ruminiclostridium* while increased *Klebsiella* and *Acinetobacter* are responsible for the activation of the HPA axis, namely increased levels of CRH, ACTH and corticosterone. *Ruminiclostridium* can ferment cellulose, cellobiose, glucose and xylose for producing acetate (Zhang *et al*., 2018), which has neural activity and reaches the central nervous system (CNS) to relieve the activation of the HPA axis (Cryan *et al*., 2019). Further, Widmaier and Katoh also demonstrate that acetate inhibits hormone release of the HPA axis both *in vivo* and *in vitro* (Widmaier *et al*., 1995; Katoh *et al*., 2004). On

the contrary, *Klebsiella* and *Acinetobacter* promote inflammatory cytokines release that in turn activate the HPA axis (Cryan *et al*., 2019). Moreover, these three genera also contribute to the serum level of insulin, NEFA, BUN, and creatine, which may be related to the activation of the HPA axis. Chen's study supports that hypoxic stress reduces plasma glucose and insulin levels, while increases glucagon levels by activating the HPA axis (CRH receptor) in rats (Chen *et al*., 2007). We speculate that late gestational HS in our study intensifies the HPA axis response by regulating gut microbiota (i.e. Ruminococcaceae, Lachnospiraceae and γ-Proteobacteria), which strengthens fat and protein catabolism to maintain energy requirement for both mom and her fetus (Havel and Taborsky, 1989).

Based on the endosymbiosis theory, mitochondria of eukaryotic cells are evolved from α-Proteobacteria and are considered as the descendants of bacteria (Bajpai *et al*., 2018). We further explore the potential microbial drivers to mRNA expression of hepatic mitochondrial functional genes. Our results indicate that, compared with nuclear-encoded genes, mtDNA-encoded genes are more susceptible to bacterial alterations. *Ruminiclostridium* mainly produces acetate and hydrogen (Zhang *et al*., 2018). Acetate enters the liver through the portal vein and continues to metabolize, which is related to the energy metabolism and biosynthesis of mitochondria (Clark and Mach, 2017). Hydrogen can effectively neutralize the ROS generated by the mitochondrial respiratory chain for reducing mitochondrial oxidative damage (Cui *et al*., 2014). Moreover, potential pathogens such as *Klebsiella*, *Escherichia–Shigella* and *Acinetobacter* can activate the NF-κB signal pathway to promote inflammation by producing LPS binding to Toll-like receptor 4 (TLR-4), which in turn promote ROS production and oxidative damage of mitochondrial respiratory chain (Saint-Georges-Chaumet and Edeas, 2016). According to these results, we speculated that hepatic mitochondrial dysfunction has strongly associated with gut microbial dysbiosis due to late gestational HS.

This study did have limitations. First, the 16S rRNA gene sequencing we used to provide low resolution at the species level and poor discriminatory power for some genera, whole-metagenome shotgun sequencing should be applied for higher strain-level resolution and more accurate information regarding the microbial composition and function in further study. Moreover, although we used the random forest algorithm and multiple linear regression to predict the contribution of potential microbial drivers for mitochondrial function and metabolic profiles, our findings are correlational and do not support a causal relationship between gut microbiota and hepatic mitochondrial function. Faecal microbiota transplantation (FMT) should be applied to elucidate the underlying causality in future studies. Nevertheless, our data provide evidence for the relationship between gut microbiota and hepatic mitochondrial function involved in the disrupted glycolipid metabolism during late gestational HS, which in turn provides new insight into the potential risk of gestational high ambient temperature exposure and may further present basic data on the possible mechanism of gestational HS on human health. More studies are needed to determine the further mechanism of gut microbiota that is involved in energy homeostasis to prevent metabolic syndrome during pregnancy.

Experimental procedures

Animals, experimental design and sampling

Twenty female and ten male mice, both Institute of Cancer Research (ICR) mice aged 6 weeks (20 ± 2 g), were purchased from the Model Animal Research Center of Nanjing University (Nanjing, China) and housed in the Laboratory Animal Center of Nanjing Agricultural University (Nanjing, China). The sample size of this experiment was predetermined according to the previous method (Noordzij *et al*., 2010). Mice were housed and maintained at conditions of 24 ± 2°C and a 12 h light/dark cycle with *ad libitum* access water and a standard chow diet. After three days of adaptation, one male and two female mice were housed in each cage from 7:00 p.m. to 7:00 a.m. daily for successful mating. Pregnant mice were moved into separate cages once the pregnancy was determined via a vaginal plug the following morning. The day when the vaginal plug appeared was defined as the first day of gestation. The animal experiments were approved by the Animal Welfare and Use Committee of Nanjing Agricultural University and were implemented following Animal Research Institute Committee Guidelines (Nanjing, China, SYXK (Su) 2011-0036).

Twenty pregnant mice were randomly assigned into two environmental treatments including the TN (24 ± 2 °C; n = 10) and HS (35 ± 2 °C; n = 10) conditions from d 12 of gestation. A randomized complete block design was present here based on their body weight as previously described (Gao *et al*., 2019). Note that this method aimed to eliminate differences in performance among groups. Rectal temperature, feed intake and water consumption were monitored at 8:00 a.m. every morning. Body weight was only recorded during the experimental treatment period. After 12 h of starvation, pregnant mice were euthanized with pentobarbital sodium for blood, tissue and colonic digesta samples collections at d 18 of gestation. Blood samples were collected from the retro-orbital plexus using a collection tube with gel & clot activator (Kangjie equipment & supply Co., Ltd, Jiangsu, China). The serum sample was centrifuged at 3000 g for 15 min at 4 °C, then collected and frozen at −20°C

before analysis. The livers, heart, lung, pancreas, small and large intestine, gastrocnemius muscle, and abdominal and subcutaneous fat were collected for calculating the visceral index as previously reported (Dong *et al*., 2017). Parts of livers were collected and stored in liquid nitrogen and then stored at −80°C before RNA isolation. For body composition, carcass nitrogen and fat contents were measured as described previously (Park *et al*., 1999). The colonic digesta samples were collected from the colon immediately and aseptically transferred into a 2 ml sterile tube and stored at −80°C for further DNA extraction. Two mice of the HS group were excluded from further analysis due to stillbirth before sample collection. Hence, we have 10 samples in TN group and 8 samples in HS group for further analysis respectively.

Hormones and metabolites assays

Serum hormones and metabolites of pregnant mice were determined by the commercial enzyme-linked immunosorbent assay (ELISA) kit according to their instructions strictly (Fangcheng Beijing Technology Co. Ltd., Beijing, China). CRH, ACTH, corticosterone, Hsp70, IGF-1, insulin, glucagon, NEFA, B-HBA, BUN, creatinine, MDA and 8-OHdG levels were detected in mice serum, with assay sensitivities above 0.1 $pg{\cdot}ml^{-1}$, 0.1 $pg{\cdot}ml^{-1}$, 1.0 $ng{\cdot}l^{-1}$, 1.0 $pg{\cdot}ml^{-1}$, 0.1 $ng{\cdot}ml^{-1}$, 0.1 $mIU{\cdot}l^{-1}$, 1.0 $mU{\cdot}l^{-1}$, 1.0 μM, 1.0 μM, 0.1 mM, 1.0 μM, 1 $nmol{\cdot}ml^{-1}$ and 1 $ng{\cdot}ml^{-1}$ respectively. The intra- and inter-assay coefficients of variations for all measures were 10% and 15% respectively. Moreover, serum levels of glucose, cholesterol, TG, high-density lipoprotein (HDL) and low-density lipoprotein (LDL) were measured with an automatic biochemical analyzer (Hitachi 7180; Hitachi High-Technologies Co., Tokyo, Japan) using corresponding commercial kits (MedicalSystem Biotechnology Co., Ltd., Ningbo, China).

Quantitative reverse transcription PCR (qRT-PCR)

qRT-PCR was performed according to a previous study (Ji *et al*., 2019). Total RNA from the liver was extracted and then reverse-transcribed to the complementary DNA (cDNA). qRT-PCR of the target genes was performed using a QuantStudio 5 Real-Time PCR System (Thermo Fisher, USA) with fluorescence detection of TB green dye (TaKaRa Bio Co., Ltd., Beijing, China). The target genes are all mitochondrial functional genes, which mainly included 13 mtDNA-encoded genes and several nuclear-encoded genes. All the primers were synthesized by Invitrogen Life Technologies (Invitrogen Co., Ltd., Shanghai, China) with their sequences shown in Table S2. The relative mRNA expression levels were calculated using the $2^{-\Delta\Delta Ct}$ method described previously (Livak and Schmittgen, 2001).

DNA extraction, MiSeq sequencing and Bioinformatics analysis

The total genomic DNA of colonic digesta samples was extracted as described previously (He *et al*., 2019a). Successively, the V3-V4 hypervariable region of bacterial 16S rDNA was amplified using a universal forward primer 341F (5'-CCTAYGGGRBGCASCAG-3') and a reverse primer 806R (5'-GGACTACNNGGGTATCTAAT-3'). Purified amplicons were pooled in equimolar and paired-end sequenced (2 × 250) on an Illumina MiSeq platform by Biozeron Biotechnology (Shanghai, China) (Caporaso *et al*., 2012). The raw reads were deposited into the NCBI Sequence Read Archive (SRA) database (Accession Number: SRP287964).

Raw data generated from 16S rRNA MiSeq sequencing were analysed as a previous study (He *et al*., 2019a). The phylum and OTU with relative abundance higher than 1% and 0.1%, respectively, were defined as predominant and sorted for further comparison. Interactive tree of life (iTOL) plots were generated as phylogenetic trees based on the relative abundance of differential OTU (Letunic and Bork, 2019). Microbial functions were predicted based on the 16S rDNA sequence using PICRUSt (Langille *et al*., 2013).

Statistical analysis

Power calculations identified the sample size is enough to detect an effect size of 1.42 SD for the data with 80% power and a type I error of 5% by using G*Power Data Analysis (Faul *et al*., 2007). Statistical analyses were performed using SPSS 26.0 software (IBM Inc., Chicago, IL, USA). Two-way ANOVA was used to analyse the effects of HS and time on the rectal temperature, feed intake, water consumption and body weight, considering the HS on those parameters as the main effect. Serum hormones and metabolites, carcass fat and protein contents, as well as mitochondrial functional gene expression, were assessed for normal distribution with the Shapiro–Wilk test. Student's t-test or the non-parametric Mann–Whitney *U*-test was applied to compare the difference between groups. Data were expressed as the mean ± SEM or median. Differences in the bacterial α-diversity indices and the relative abundance (phylum and OTU levels) were analysed using the non-parametric Mann–Whitney *U*-test. Data were expressed as medians, and the *q* value was calculated based on the *P*-value with false discovery rate FDR correction (Benjamini and Hochberg, 1995), and $q < 0.05$ was regarded as statistically different. Principal coordinate analysis (PCoA) plot

based on the unweighted_unifrac distance metric was used to visualize the difference in bacterial β-diversity. Bacterial community structure comparison was evaluated by permutational multivariate analysis of variance (PERMANOVA), using the 'vegan' package in R (http://www.r-project.org/). The differences were significant in all the above tests at $P < 0.05$. Additionally, the potential microbial drivers for the significant differential serum metabolites and mitochondrial functional genes were identified as described previously (He *et al*., 2020).

Acknowledgements

This work was supported by the National Key R&D Program of China (2016YFD0500502), the earmarked fund for Jiangsu Modern Agricultural (Swine) Industry Technology System (JATS[2020]412) and the Startup Fund for Newly Advanced Doctoral Research of Shaanxi University of Chinese Medicine (303-17102032039). The authors also would like to thank Shanghai Biozeron Biotechnology Co., Ltd for its assistance in the original data processing and related bioinformatics analysis of MiSeq sequencing. Additionally, Dr. He would like to particularly thank his family, for their overflowing love and support.

Funding Information

This work was supported by the National Key R&D Program of China (2016YFD0500502), the earmarked fund for Jiangsu Modern Agricultural (Swine) Industry Technology System (JATS[2020]412) and the Startup Fund for Newly Advanced Doctoral Research of Shaanxi University of Chinese Medicine (303-17102032039).

Conflict of interest

The authors declare no conflicts of interest.

References

Abrams, B. (2021) Maternal undernutrition and reproductive performance. In *Infant and Child Nutrition Worldwide*. Boca Raton, FL: CRC Press, pp. 31–60.

Aggarwal, A., and Upadhyay, R. (2012) *Heat Stress and Animal Productivity*. Switzerland AG: Springer Science & Business Media,

Bajpai, P., Darra, A., and Agrawal, A. (2018) Microbe-mitochondrion crosstalk and health: an emerging paradigm. *Mitochondrion* **39:** 20–25.

Basu, R., Chen, H., Li, D.-K., and Avalos, L.A. (2017) The impact of maternal factors on the association between temperature and preterm delivery. *Environ Res* **154:** 109–114.

Belhadj Slimen, I., Najar, T., Ghram, A., and Abdrrabba, M. (2016) Heat stress effects on livestock: molecular, cellular and metabolic aspects, a review. *J Anim Physiol Anim Nutr (Berl)* **100:** 401–412.

Bellance, N., Lestienne, P., and Rossignol, R. (2009) Mitochondria: from bioenergetics to the metabolic regulation of carcinogenesis. *Front Biosci (Landmark Ed)* **14:** 4015–4034.

Beltran, A.J., Wu, J., and Laurent, O. (2014) Associations of meteorology with adverse pregnancy outcomes: a systematic review of preeclampsia, Preterm birth and birth weight. *Int J Env Res Pub He* **11:** 91–172. https://doi.org/10.3390/ijerph110100091

Benjamini, Y., and Hochberg, Y. (1995) Controlling the false discovery rate: a practical and powerful approach to multiple testing. *J R Stat Soc B* **57:** 289–300. https://doi.org/10.1111/j.2517-6161.1995.tb02031.x

Biddle, A., Stewart, L., Blanchard, J., and Leschine, S. (2013) Untangling the genetic basis of fibrolytic specialization by lachnospiraceae and ruminococcaceae in diverse gut communities. *Diversity* **5:** 627–640. https://doi.org/10.3390/d5030627

Cadenas, E., and Davies, K.J.A. (2000) Mitochondrial free radical generation, oxidative stress, and aging. *Free Radical Bio Med* **29:** 222–230. https://doi.org/10.1016/S0891-5849(00)00317-8

Caporaso, J.G., Lauber, C.L., Walters, W.A., Berg-Lyons, D., Huntley, J., Fierer, N., *et al*. (2012) Ultra-high-throughput microbial community analysis on the Illumina HiSeq and MiSeq platforms. *ISME J* **6:** 1621–1624.

Chen, X.Q., Dong, J., Niu, C.Y., Fan, J.M., and Du, J.Z. (2007) Effects of hypoxia on glucose, insulin, glucagon, and modulation by corticotropin-releasing factor receptor type 1 in the rat. *Endocrinology* **148:** 3271–3278.

Clark, A., and Mach, N. (2017) The crosstalk between the gut microbiota and mitochondria during exercise. *Front Physiol* **8:** 319.

Compare, D., Coccoli, P., Rocco, A., Nardone, O.M., De Maria, S., Cartenì, M., and Nardone, G. (2012) Gut–liver axis: The impact of gut microbiota on non alcoholic fatty liver disease. *Nutr Metab Cardiovas* **22:** 471–476.

Cryan, J.F., O'Riordan, K.J., Cowan, C.S.M., Sandhu, K.V., Bastiaanssen, T.F.S., Boehme, M., *et al*. (2019) The Microbiota-gut-brain axis. *Physiol Rev* **99:** 1877–2013.

Cui, Y., Zhang, H., Ji, M., Jia, M., Chen, H., Yang, J., and Duan, M. (2014) Hydrogen-rich saline attenuates neuronal ischemia–reperfusion injury by protecting mitochondrial function in rats. *J Surg Res* **192:** 564–572. https://doi.org/10.1016/j.jss.2014.05.060

Diebold, L., and Chandel, N.S. (2016) Mitochondrial ROS regulation of proliferating cells. *Free Radical Bio Med* **100:** 86–93.

Dong, Z., Xu, M., Huang, J., Chen, L., Xia, J., Chen, X., *et al*. (2017) The protective effect of Ginsenoside Rg1 on aging mouse pancreas damage induced by D-galactose. *Exp Ther Med* **14:** 616–622.

Du, J., Di, H.-S., Guo, L., Li, Z.-H., and Wang, G.-L. (2008) Hyperthermia causes bovine mammary epithelial cell death by a mitochondrial-induced pathway. *J Therm Biol* **33:** 37–47. https://doi.org/10.1016/j.jtherbio.2007.06.002

Echtay, K.S., Roussel, D., St-Pierre, J., Jekabsons, M.B., Cadenas, S., Stuart, J.A., *et al*. (2002) Superoxide activates mitochondrial uncoupling proteins. *Nature* **415:** 96–99.

Farge, G., Mehmedovic, M., Baclayon, M., Wildenberg, S.M.J.L.v.d., Roos, W.H., and Gustafsson, C.M. *et al*. (2014) In vitro-reconstituted nucleoids can block mitochondrial dna replication and transcription. *Cell Rep* **8:** 66-74.

Faul, F., Erdfelder, E., Lang, A.G., and Buchner, A. (2007) G*Power 3: a flexible statistical power analysis program for the social, behavioral, and biomedical sciences. *Behav Res Methods* **39:** 175–191.

Galsgaard, K.D., Pedersen, J., Knop, F.K., Holst, J.J., and Wewer Albrechtsen, N.J. (2019) Glucagon receptor signaling and lipid metabolism. *Front Physiol* **10:** 413.

Gao, K., Pi, Y., Mu, C.L., Farzi, A., Liu, Z., and Zhu, W.Y. (2019) Increasing carbohydrate availability in the hindgut promotes hypothalamic neurotransmitter synthesis: aromatic amino acids linking the microbiota-brain axis. *J Neurochem* **149:** 641–659.

Gao, L.M., Zhou, T.T., Chen, Z.P., Wassie, T., Li, B., Wu, X., and Yin, Y.L. (2021) Maternal yeast-based nucleotide supplementation decreased stillbirth by regulating nutrient metabolism. *J Sci Food Agric* **101:** 4018–4032.

Gohir, W., Whelan, F.J., Surette, M.G., Moore, C., Schertzer, J.D., and Sloboda, D.M. (2015) Pregnancy-related changes in the maternal gut microbiota are dependent upon the mother's periconceptional diet. *Gut Microbes* **6:** 310–320.

Gonzalez-Rivas, P.A., Chauhan, S.S., Ha, M., Fegan, N., Dunshea, F.R., and Warner, R.D. (2019) Effects of heat stress on animal physiology, metabolism, and meat quality: a review. *Meat Sci* **162:** 108025. https://doi.org/10.1016/j.meatsci.2019.108025.

Harikai, N., Tomogane, K., Miyamoto, M., Shimada, K., Onodera, S., and Tashiro, S.-I. (2003) Dynamic responses to acute heat stress between 34°C and 38.5°C, and characteristics of heat stress response in mice. *Biol Pharm Bull* **26:** 701–708.

Hauck, C.R., and Ohlsen, K. (2006) Sticky connections: extracellular matrix protein recognition and integrin-mediated cellular invasion by *Staphylococcus aureus*. *Curr Opin in Microbiol* **9:** 5–11.

Havel, P.J., and Taborsky, G.J. Jr (1989) The contribution of the autonomic nervous system to changes of glucagon and insulin secretion during hypoglycemic stress. *Endocr Rev* **10:** 332–350.

He, J., Guo, H., Zheng, W., Xue, Y., Zhao, R., and Yao, W. (2019a) Heat stress affects fecal microbial and metabolic alterations of primiparous sows during late gestation. *J Anim Sci Biotechnol* **10:** 84. https://doi.org/10.1186/s40104-019-0391-0

He, J., Zheng, W., Lu, M., Yang, X., Xue, Y., and Yao, W. (2019b) A controlled heat stress during late gestation affects thermoregulation, productive performance, and metabolite profiles of primiparous sow. *J Therm Biol* **81:** 33–41. https://doi.org/10.1016/j.jtherbio.2019.01.011

He, J., Zheng, W., Tao, C., Guo, H., Xue, Y., Zhao, R., and Yao, W. (2020) Heat stress during late gestation disrupts maternal microbial transmission with altered offspring's gut microbial colonization and serum metabolites in a pig model. *Environ Pollut* **266:** 115111.

He, X., Lu, Z., Ma, B., Zhang, L., Li, J., Jiang, Y., *et al*. (2018) Effects of chronic heat exposure on growth performance, intestinal epithelial histology, appetite-related hormones and genes expression in broilers. *J Sci Food Agric* **98:** 4471–4478.

Hsiang, S., Kopp, R., Jina, A., Rising, J., Delgado, M., Mohan, S., *et al*. (2017) Estimating economic damage from climate change in the United States. *Science* **356:** 1362–1369.

Ji, X., Zhang, Q., Zheng, W., and Yao, W. (2019) Morphological and molecular response of small intestine to lactulose and hydrogen-rich water in female piglets fed *Fusarium mycotoxins* contaminated diet. *J Anim Sci Biotechnol* **10:** 9.

Kakiyama, G., Pandak, W.M., Gillevet, P.M., Hylemon, P.B., Heuman, D.M., Daita, K., *et al*. (2013) Modulation of the fecal bile acid profile by gut microbiota in cirrhosis. *J Hepatol* **58:** 949–955.

Karl, J.P., Hatch, A.M., Arcidiacono, S.M., Pearce, S.C., Pantoja-Feliciano, I.G., Doherty, L.A., and Soares, J.W. (2018) Effects of psychological, environmental and physical stressors on the gut microbiota. *Front Microbiol* **9:** 2013.

Katoh, K., Asari, M., Ishiwata, H., Sasaki, Y., and Obara, Y. (2004) Saturated fatty acids suppress adrenocorticotropic hormone (ACTH) release from rat anterior pituitary cells in vitro. *Comp Biochem Physiol A Mol Integr Physiol* **137:** 357–364.

Kilinc, M.F., Cakmak, S., Demir, D.O., Doluoglu, O.G., Yildiz, Y., Horasanli, K., and Dalkilic, A. (2016) Does maternal exposure during pregnancy to higher ambient temperature increase the risk of hypospadias? *J Pediatr Urol* **12:** 407.e401–407.e406.

Koh, H. (2016) Communicating the health effects of climate change. *JAMA* **315:** 239–240.

Koren, O., Goodrich, J.K., Cullender, T.C., Spor, A., Laitinen, K., Kling Bäckhed, H., *et al*. (2012) Host remodeling of the gut microbiome and metabolic changes during pregnancy. *Cell* **150:** 470–480.

Krautkramer, K.A., Fan, J., and Backhed, F. (2020) Gut microbial metabolites as multi-kingdom intermediates. *Nat Rev Microbiol* **19:** 77–94.

Lagkouvardos, I., Lesker, T.R., Hitch, T.C.A., Gálvez, E.J.C., Smit, N., Neuhaus, K., *et al*. (2019) Sequence and cultivation study of Muribaculaceae reveals novel species, host preference, and functional potential of this yet undescribed family. *Microbiome* **7:** 28.

Lambert, G.P. (2009) Stress-induced gastrointestinal barrier dysfunction and its inflammatory effects. *J Anim Sci* **87:** E101–E108.

Langille, M.G.I., Zaneveld, J., Caporaso, J.G., McDonald, D., Knights, D., Reyes, J.A., *et al*. (2013) Predictive functional profiling of microbial communities using 16S rRNA marker gene sequences. *Nat Biotechnol* **31:** 814–821.

Letunic, I., and Bork, P. (2019) Interactive Tree Of Life (iTOL) v4: recent updates and new developments. *Nucleic Acids Res* **47:** W256–W259.

Li, T., Gao, J., Du, M., and Mao, X. (2019) Bovine alpha-lactalbumin hydrolysates ameliorate obesity-associated

endotoxemia and inflammation in high-fat diet-fed mice through modulation of gut microbiota. *Food Funct* **10:** 3368–3378.

Liao, Y., Hu, R., Wang, Z., Peng, Q., Dong, X., Zhang, X., *et al*. (2018) Metabolomics profiling of serum and urine in three beef cattle breeds revealed different levels of tolerance to heat stress. *J agr Food Chem* **66:** 6926–6935.

Liu, J., Hao, W., He, Z., Kwek, E., Zhao, Y., Zhu, H., *et al*. (2019) Beneficial effects of tea water extracts on the body weight and gut microbiota in C57BL/6J mice fed with a high-fat diet. *Food Funct* **10:** 2847–2860.

Liu, S.S., and Li, Y. (2009) Regulation of mitochondrial genes transcription in mammalian cells. *Chin J Cell Biol* **31:** 811–816.

Livak, K.J., and Schmittgen, T.D. (2001) Analysis of relative gene expression data using real-time quantitative PCR and the $2-\Delta\Delta$CT method. *Methods* **25:** 402–408. https://doi.org/10.1006/meth.2001.1262

Lof, M., Olausson, H., Bostrom, K., Janerot-Sjöberg, B., Sohlstrom, A., and Forsum, E. (2005) Changes in basal metabolic rate during pregnancy in relation to changes in body weight and composition, cardiac output, insulin-like growth factor I, and thyroid hormones and in relation to fetal growth. *Am J Clin Nutr* **81:** 678–685.

Lu, Z., He, X., Ma, B., Zhang, L., Li, J., Jiang, Y., *et al*. (2017) Chronic heat stress impairs the quality of breast-muscle meat in broilers by affecting redox status and energy-substance metabolism. *J Agric Food Chem* **65:** 11251–11258.

Ma, W., Wang, L., Lin, H., Liu, T., Zhang, Y., Rutherford, S., *et al*. (2015) The temperature–mortality relationship in China: an analysis from 66 Chinese communities. *Environ Res* **137:** 72–77. https://doi.org/10.1016/j.envres.2014.11.016

Mailloux, R.J., and Harper, M.E. (2011) Uncoupling proteins and the control of mitochondrial reactive oxygen species production. *Free Radic Biol Med* **51:** 1106–1115.

Mella, M.T., Kohari, K., Jones, R., Pena, J., Ferrara, L., Stone, J., and Lambertini, L. (2016) Mitochondrial gene expression profiles are associated with intrahepatic cholestasis of pregnancy. *Placenta* **45:** 16–23.

Morera, P., Basirico, L., Hosoda, K., and Bernabucci, U. (2012) Chronic heat stress up-regulates leptin and adiponectin secretion and expression and improves leptin, adiponectin and insulin sensitivity in mice. *J Mol Endocrinol* **48:** 129–138.

Mujahid, A., Akiba, Y., and Toyomizu, M. (2007b) Acute heat stress induces oxidative stress and decreases adaptation in young white leghorn cockerels by downregulation of avian uncoupling protein. *Poult Sci* **86:** 364–371.

Mujahid, A., Pumford, N.R., Bottje, W., Nakagawa, K., Miyazawa, T., Akiba, Y., and Toyomizu, M. (2007a) Mitochondrial oxidative damage in chicken skeletal muscle induced by acute heat stress. *J Poult Sci* **44:** 439–445. https://doi.org/10.2141/jpsa.44.439

Nasiri, R., Ahmadi Shadmehri, A., Khajeh Ghiassi, P., Sarafraz Yazdi, M., and Mazloum Farsi Baf, M. (2014) Association of meteorological factors and seasonality with preeclampsia: a 5-year study in northeast of Iran. *Clin Exp Hypertens* **36:** 586–589.

Nelson, L. D., and Cox, M. M. (2017) *Lehninger Principles of Biochemistry*. 7th ed., New York: W. H. Freeman & Co.

Nicholson, J.K., Holmes, E., Kinross, J., Burcelin, R., Gibson, G., Jia, W., and Pettersson, S. (2012) Host-gut microbiota metabolic interactions. *Science* **336:** 1262–1267.

NOAA (2020) *National Centers for Environmental Information, State of the Climate: National Climate Report for Annual*. Washington, DC: NOAA.

Noordzij, M., Tripepi, G., Dekker, F.W., Zoccali, C., Tanck, M.W., and Jager, K.J. (2010) Sample size calculations: basic principles and common pitfalls. *Nephrol Dial Transplant* **25:** 1388–1393.

Ormerod, K.L., Wood, D.L.A., Lachner, N., Gellatly, S.L., Daly, J.N., Parsons, J.D., *et al*. (2016) Genomic characterization of the uncultured Bacteroidales family S24–7 inhabiting the guts of homeothermic animals. *Microbiome* **4:** 36.

Papacleovoulou, G., Nikolova, V., Oduwole, O., Chambers, J., Vazquez-Lopez, M., Jansen, E., *et al*. (2017) Gestational disruptions in metabolic rhythmicity of the liver, muscle, and placenta affect fetal size. *FASEB J* **31:** 1698–1708.

Park, Y., Storkson, J.M., Albright, K.J., Liu, W., and Pariza, M.W. (1999) Evidence that the trans-10, cis-12 isomer of conjugated linoleic acid induces body composition changes in mice. *Lipids* **34:** 235–241. https://doi.org/10.1007/s11745-999-0358-8

Pearce, S.C., Gabler, N.K., Ross, J.W., Escobar, J., Patience, J.F., Rhoads, R.P., and Baumgard, L.H. (2013) The effects of heat stress and plane of nutrition on metabolism in growing pigs. *J Anim Sci* **91:** 2108–2118.

Saint-Georges-Chaumet, Y., and Edeas, M. (2016) Microbiota-mitochondria inter-talk: consequence for microbiota-host interaction. *Pathog Dis* **74:** ftv096.

Sharma, A.X., Quittner-Strom, E.B., Lee, Y., Johnson, J.A., Martin, S.A., Yu, X., *et al*. (2018) Glucagon receptor antagonism improves glucose metabolism and cardiac function by promoting AMP-mediated protein kinase in diabetic mice. *Cell Rep* **22:** 1760–1773.

Shi, R.L., and Jiang, L.L. (2009) Recent advances in peroxisomal fatty acid β-oxidation. *Chin J Biochem Mole Biol* **25:** 12–16.

Sommer, F., and Bäckhed, F. (2013) The gut microbiota—masters of host development and physiology. *Nat rev microbiol* **11:** 227–238.

Sridharan, V., Guichard, J., Li, C.-Y., Muise-Helmericks, R., Beeson, C.C., and Wright, G.L. (2008) O2-sensing signal cascade: clamping of O2 respiration, reduced ATP utilization, and inducible fumarate respiration. *Am J physiol-Cell Ph* **295:** C29–C37. https://doi.org/10.1152/ajpcell.00466.2007

Strand, L.B., Barnett, A.G., and Tong, S. (2011) The influence of season and ambient temperature on birth outcomes: a review of the epidemiological literature. *Environ Res* **111:** 451–462.

Widmaier, E.P., Margenthaler, J., and Sarel, I. (1995) Regulation of pituitary-adrenocortical activity by free fatty acids in vivo and in vitro. *Prostag Leukotr Ess* **52:** 179–183.

Xue, Y., Guo, C., Hu, F., Zhu, W., and Mao, S. (2019) Maternal undernutrition induces fetal hepatic lipid metabolism disorder and affects the development of fetal liver in a sheep model. *FASEB J* **33:** 9990–10004.

Yang, J., Yin, P., Zhou, M., Ou, C.-Q., Guo, Y., Gasparrini, A., *et al*. (2015) Cardiovascular mortality risk attributable to ambient temperature in China. *Heart* **101:** 1966–1972.

Yoneyama, M., and Fujita, T. (2009) RNA recognition and signal transduction by RIG-I-like receptors. *Immunol Rev* **227:** 54–65.

Zhang, X., Tu, B.o., Dai, L.-R., Lawson, P.A., Zheng, Z.-Z., Liu, L.-Y., *et al*. (2018) *Petroclostridium xylanilyticum* gen. nov., sp. nov., a xylan-degrading bacterium isolated from an oilfield, and reclassification of clostridial cluster III members into four novel genera in a new *Hungateiclostridiaceae* fam. nov. *Int J Syst Evol Microbiol* **68:** 3197–3211.

Zhang, Y., Yu, C., and Wang, L. (2017) Temperature exposure during pregnancy and birth outcomes: an updated systematic review of epidemiological evidence. *Environ Pollut* **225:** 700–712.

Zhou, X., Yang, H., Yan, Q., Ren, A.o., Kong, Z., Tang, S., *et al*. (2019) Evidence for liver energy metabolism programming in offspring subjected to intrauterine undernutrition during midgestation. *Nutr Metab (Lond)* **16:** 20.

Supporting information

Additional supporting information may be found online in the Supporting Information section at the end of the article.

Fig. S1. Effects of heat stress during late gestation on the serum levels of Hsp70 (A) and HPA axis hormones (B-D) of pregnant mice. The data are presented as the mean ± SEM. Asterisks (**, ***) means the significant difference between TN and HS group ($P < 0.01$, $P < 0.001$). ACTH: adrenocorticotropic hormone; CRH: corticotropin-releasing hormone; HPA: Hypothalamus pituitary adrenal; HS = heat stress; Hsp = heat shock protein; TN = thermoneutral.

Fig. S2. Effects of HS during late gestation on rectal temperature (A), feed intake (B), and water consumption (C) of pregnant mice. The data are presented as the mean ± SEM. Asterisks (#, *, **, ****) means the tendency or significant difference between TN and HS group ($P < 0.10$, $P < 0.05$, $P < 0.01$, $P < 0.0001$). HS = heat stress; TN = thermoneutral; Trt: treatment.

Fig. S3. Effects of HS during late gestation on the serum levels of intestinal integrity biomarkers of pregnant mice. Asterisks (**) means the significant difference between TN and HS group ($P < 0.01$). HS = heat stress; LBP: LPS binding protein; LPS: Lipopolysaccharide; TN = thermoneutral.

Table S1. Effects of late gestational heat stress on the visceral indices of pregnant mice.

Table S2. The sequence of primers used in the qPCR.

Table S3. Effects of HS during late gestation on the colonic microbial α-diversity of pregnant mice.

Table S4. Effects of HS during late gestation on the colonic bacterial functional prediction of KEGG metabolic pathways of pregnant mice.

